J. Fluid Mech. (2007), *vol.* 579, *pp.* 373–382.
doi:10.1017/S0022112007005484 Printed in the United Kingdom

A shallow-water model for high-Reynolds-number gravity currents for a wide range of density differences and fractional depths

MARIUS UNGARISH

Department of Computer Science, Technion, Haifa 32000, Israel

(Received 19 October 2006 and in revised form 8 February 2007)

We consider the propagation of a gravity current of density ρ_c from a lock of length x_0 and height h_0 into an ambient fluid of density ρ_a in a channel of height H. When the Reynolds number is large, the resulting flow is governed by the parameters ρ_c/ρ_a and $H^* = H/h_0$. We show that the shallow-water one-layer model, combined with a Benjamin-type front condition, provides a versatile formulation for the thickness and speed of the current, without any adjustable constants. The results cover in a continuous manner the range of light $\rho_c/\rho_a \ll 1$, Boussinesq $\rho_c/\rho_a \approx 1$, and heavy $\rho_c/\rho_a \gg 1$ currents in a fairly wide range of depth ratio. We obtain analytical solutions for the initial dam-break or slumping stage of propagation with constant speed, and derive explicitly the trends for small and large values of the governing parameters. This reveals the main features: (*a*) the heavy current propagates faster and its front is thinner than for the light counterpart; (*b*) the speed of the heavy current depends little on H^*, while that of the light current increases with H^*; and (*c*) in the shallow ambient case (H^* close to 1) the light current is choked to move with the thickness of half-channel, while the heavy current typically moves with an unrestricted smaller thickness. These qualitative predictions are in accord with previous observations, and some quantitative comparisons with available experimental and numerical simulations data also show fair agreement. However, given the paucity of the available data, the main deficiency of the model is the unknown practical limit of applicability. For large time, t, a self-similar propagation with $t^{2/3}$ is feasible for both the heavy and light currents, but the thickness profiles display differences.

1. Introduction

We consider the propagation of a gravity current of density ρ_c into an ambient fluid of density ρ_a in a channel of height H. When $\rho_c/\rho_a > 1$ we refer to a heavy (dense, bottom) current and when $\rho_c/\rho_a < 1$ we refer to a light (ceiling, top) current. (Note that the terms light or heavy are with respect to the ambient.) The current is released from a lock (of length x_0 and height h_0) adjacent to the horizontal boundary on which it will spread out, illustrated in figure 1. We assume that the Reynolds number $u_N h_0/\nu$ is large and hence viscous effects can be discarded (here u_N is the speed of the nose and ν is the representative kinematic viscosity of the fluids). It is well known that in the Boussinesq case $\rho_c/\rho_a \approx 1$ the light and heavy currents display the same behaviour, i.e. in the configuration of figure 1 the bottom and top Boussinesq currents would appear as mirror images with respect to the horizontal boundary (but note that our figure emphasizes the lack of symmetry). The Boussinesq currents depend

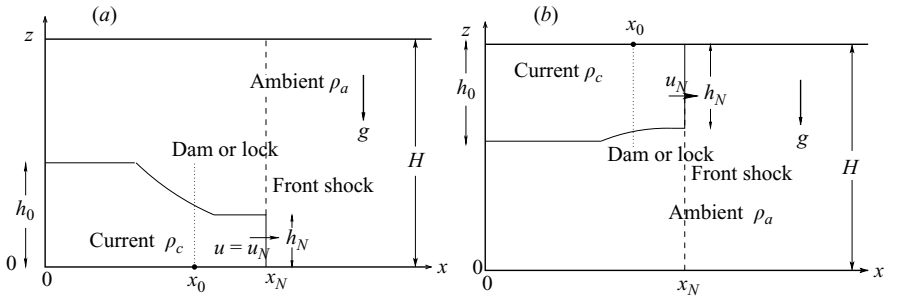

FIGURE 1. Schematic description of the (*a*) heavy and (*b*) light current released from a lock of length x_0 and height h_0 into an ambient of height H.

on one parameter only, the depth ratio

$$H^* = \frac{H}{h_0}, \tag{1.1}$$

which can be in the range $[1, \infty)$. This is not an easy problem in general, but there is a solid body of knowledge and well developed prediction tools for this current in the two-dimensional case (see Klemp, Rotunno & Skamarock 1994; Ungarish & Zemach 2005 where additional references are given). The non-Boussinesq flow is more complicated. First, mathematical difficulty is introduced because the propagation depends on an additional parameter, the density ratio ρ_c/ρ_a, which theoretically is in the range $(0, \infty)$. (We exclude from our direct analysis the special $\rho_a = 0$ case of a liquid propagating freely into a gas or vacuum, see for example Stansby, Chegini & Barnes 1998; Hogg & Pritchard 2004). Second, setting up experiments or simulations with fluids of significantly different densities requires more resources than the relatively simple water–saline systems used for the Boussinesq cases. Fanneløp & Jacobsen (1984), Keller & Chyou (1991), Gröbelbauer, Fanneløp & Britter (1993), Lowe, Rottman & Linden (2005), Birman, Martin & Meiburg (2005) and Etienne, Hopfinger & Saramito (2005), present theoretical, experimental, and numerical simulations results on the behaviour of the non-Boussinesq currents (and also discuss previous pertinent contributions). It is clear that the Boussinesq symmetry for light–heavy currents disappears when ρ_c/ρ_a departs from 1. However, the generalization of the available results (especially the quantitative ones) into a comprehensive theory and reliable prediction tool requires further work.

Most investigations, and the most accurate experimental and numerical data, are concerned with the full-depth lock exchange problem $H^* = 1$. It is difficult to extend these results to fractional depth configurations which may have applications in hazard prediction. The previously suggested theoretical formulations contain unspecified adjustable constants, or employ hydraulic (or box) model approximations. These models usually rely on assumed velocity and interface profiles, and employ difficult-to-justify closures (like global energy conservation). They can cover only a limited distance of propagation (for example, the constant-velocity initial phase). Other theoretical approaches have been concerned simply with deriving curve-fit formulas from numerical or experimental data, and extrapolating these results. This is useful information, but lacks physical support and does not provide sharp insights.

Our objective is to improve the theoretical modelling and predictions concerning the non-Boussinesq currents. We suggest a formulation based on clear equations of motion with realistic boundary and initial conditions, which covers a fairly wide range

of density ratio and fractional depth (with the possible exception of full-depth or nearly so configurations, which are also special cases in the Boussinesq limit). These equations can be used continuously for initial, intermediate and long times, until viscous forces become important.

2. Formulation

We consider incompressible immiscible fluids, and assume that the viscous effects are negligible (both in the interior and at the boundaries). The density of the current and of the ambient is ρ_c and ρ_a, respectively. The current propagates in the positive x-direction, and the gravitational acceleration g acts in the negative z-direction. The bottom and the top of the half-infinite channel are at $z=0$ and $z=H$. The propagating fluid is originally in a reservoir of length x_0 and height h_0 located adjacent to the boundary on which propagation occurs, i.e. the bottom for the heavy current and the top for the light current, see figure 1. The $x=0$ boundary is a rigid wall.

We use dimensional variables unless stated otherwise. The thickness of the current is $h(x,t)$ and its horizontal velocity (z-averaged) is $u(x,t)$. Initially, at $t=0$, $h=h_0$ and $u=0$. We assume a shallow current with $h_0/x_0 \ll 1$.

The continuity equation is

$$\frac{\partial h}{\partial t} + u\frac{\partial h}{\partial x} + h\frac{\partial u}{\partial x} = 0. \tag{2.1}$$

Let p denote the pressure reduced with $\rho_a g z$, and the subscripts a, c denote the current and the ambient domains. In the shallow-water (SW) approximation the pressure obeys the hydrostatic balance in the vertical direction. The one-layer model also assumes that the momentum flux in the ambient is negligible (compared to that of the current) and hence $p_a = C$. Pressure continuity $p_c = p_a$ at the interface ($z=h(x,t)$ for the heavy current and $z=H-h(x,t)$ for the light current) yields

$$p_c(x,z,t) = -\Delta\rho g z + |\Delta\rho| g h(x,t) + C_1, \tag{2.2}$$

where

$$\Delta\rho = \rho_c - \rho_a, \tag{2.3}$$

and $C_1 = C$ and $C + \Delta\rho H$ for the heavy and light currents, respectively. The z-averaged horizontal momentum equation is employed to express the balance between the inertial forces (proportional to ρ_c) and the $-\partial p_c/\partial x$ term, which is eliminated by (2.2). Here we assume that the deviation of the real horizontal velocity component from the z-averaged u is small, which is a reasonable approximation for low-viscosity fluids released from rest. We obtain

$$\frac{\partial u}{\partial t} + u\frac{\partial u}{\partial x} = -\frac{|\Delta\rho|}{\rho_c} g \frac{\partial h}{\partial x}. \tag{2.4}$$

The system (2.1) and (2.4) for $h(x,t)$ and $u(x,t)$ is hyperbolic, and the characteristic equations can be expressed as

$$\left(\frac{|\Delta\rho|}{\rho_c} g\right)^{1/2} \frac{\mathrm{d}h}{h^{1/2}} \pm \mathrm{d}u = 0 \quad \text{on} \quad \frac{\mathrm{d}x}{\mathrm{d}t} = u \pm \left(\frac{|\Delta\rho|}{\rho_c} g\right)^{1/2} h^{1/2}. \tag{2.5a, b}$$

To obtain realistic gravity current solutions the system of equations must be subjected to a boundary condition at the nose (or front) $x = x_N(t)$ (see Klemp *et al.* 1994 for a discussion). The vertical plane which moves with the nose of the inviscid

SW gravity current is treated as a discontinuity. Following Benjamin (1968), it can be shown that volume and momentum balances about the front, supplemented by the constraint that the energy in this domain cannot increase, require that the velocity of propagation must be related to the height of the current at the front by

$$u_N = \left(\frac{|\Delta\rho|}{\rho_a} g\right)^{1/2} h_N^{1/2} Fr(a), \quad \text{and} \quad a \leqslant \frac{1}{2}, \tag{2.6}$$

where N denotes the nose (front), $a = h_N/H$ and $Fr(a)$ is Benjamin's Froude number function,

$$Fr(a) = \left[\frac{(2-a)(1-a)}{1+a}\right]^{1/2}. \tag{2.7}$$

We emphasize that equations (2.1), (2.4)–(2.7) are applicable to both heavy and light currents (this is the reason for using the absolute value of $\Delta\rho$). The non-Boussinesq effect is already evident: equation (2.6) indicates that the speed of the front is proportional to $|\Delta\rho|/\rho_a$, while according to (2.4) and (2.5) the intrinsic speed of the current is proportional to $|\Delta\rho|/\rho_c$. This apparent conflict is accommodated by the thickness (representing the pressure distribution) which thus becomes a function of ρ_c/ρ_a. This interplay between speed and height is the backbone of the model. Estimates of the effect of the return flow suggest that the momentum balance (2.4) is restricted to, roughly, $H^*(\rho_c/\rho_a) > 2$, but there are indications, see below, that the model is useful beyond this bound. The other two equations of the model have a wider range of relevance and apparently restrain the global error.

An advantage of the one-layer SW model is the possibility of obtaining simple analytical solutions for the initial and fully developed phases of propagation, as described below.

3. Dam-break and initial slumping motion

The analysis of system (2.5)–(2.7) indicates that after release from the rectangular lock the current will enter a slumping phase of propagation with constant velocity over a significant distance (several lock lengths). This constant-velocity feature is shared by both Boussinesq and non-Boussinesq currents, as confirmed by experiments and numerical Navier–Stokes simulations (Gröbelbauer *et al.* 1993; Lowe *et al.* 2005; Birman *et al.* 2005; Etienne *et al.* 2005). During this slumping stage, the domain of fluid trailing the nose is a rectangle of constant height, h_N. In the absence of shocks, the velocity of propagation and the thickness h_N can be obtained analytically by matching the solution on a forward-propagating characteristic with the front condition. Integrating (2.5a) (on the + branch subject to $u = 0$ for $h = h_0$) and using (2.6) yields

$$2\left(\frac{|\Delta\rho|}{\rho_c}\right)^{1/2}\left[1 - \sqrt{\frac{h_N}{h_0}}\right](gh_0)^{1/2} = \left(\frac{|\Delta\rho|}{\rho_a}\right)^{1/2}\sqrt{\frac{h_N}{h_0}}\, Fr(a)(gh_0)^{1/2}, \tag{3.1}$$

where, again, $a = h_N/H$ and $Fr(a)$ is given by (2.7). The left-hand side is the value of u_N imposed by the characteristic, and the right-hand side is the value of u_N imposed by the front conditions. This equation provides the value of h_N/h_0; then, u_N can be calculated using either side of the equation. However, this result has physical validity only if it satisfies the restriction $a \leqslant 1/2$; otherwise, the right-hand side with $a = 1/2$ dominates, as discussed later. We expect that the left-hand side of (3.1) overestimates the value of u_N for a given h_N because the hindering effects of the return flow were not incorporated in the momentum equation.

It is convenient to express the results in dimensionless form. The velocity result will be expressed by means of an effective Froude number,

$$\chi = \frac{u_N}{(g'h_0)^{1/2}} \quad \text{where} \quad g' = \frac{|\Delta\rho|}{\max(\rho_c, \rho_a)} g. \tag{3.2}$$

The value of χ at $(\rho_c/\rho_a) = 1$ is defined as the corresponding limit, which is actually the Boussinesq limit. We obtain a continuous function of the density ratio (as expected, the right and left limits coincide, i.e. slightly heavier or lighter currents move with the same speed). The height of the nose (and of the horizontal interface which follows) will enter our results in the dimensionless combination h_N/h_0. (We note in passing that Lowe *et al.* 2005 and Birman *et al.* 2005 use a similar scaling for speed and height.) Our objective is to derive the behaviour of χ and h_N/h_0 as functions of ρ_c/ρ_a and H^*.

3.1. *Asymptotes*

We first derive analytical expressions and insights for very heavy ($\rho_c/\rho_a \gg 1$) and very light ($\rho_c/\rho_a \ll 1$) currents, and also for shallow and deep ambients ($H^* \approx 1$ and $H^* \gg 1$).

Heavy current. We rewrite (3.1) as

$$2\left(\frac{\rho_a}{\rho_c}\right)^{1/2}\left[1 - \sqrt{\frac{h_N}{h_0}}\right] = \sqrt{\frac{h_N}{h_0}}\, Fr(a). \tag{3.3}$$

For a very heavy current $\rho_a/\rho_c \to 0$ the left-hand side becomes small, and in order to balance it h_N/h_0 on the right-hand side must also be small, which also implies that $Fr(a)$ tends to $Fr(0) = \sqrt{2}$. A formal expansion of h_N/h_0 in terms of the small parameter $(\rho_a/\rho_c)^{1/2}$ yields the leading terms approximation

$$\chi = 2\left(1 - \sqrt{2\frac{\rho_a}{\rho_c}}\right), \qquad \frac{h_N}{h_0} = 2\frac{\rho_a}{\rho_c}\left(1 - 2\sqrt{2\frac{\rho_a}{\rho_c}}\right), \quad \left(\frac{\rho_a}{\rho_c} \ll 1\right). \tag{3.4}$$

Simply, as the density ratio ρ_c/ρ_a increases, the speed of propagation increases and the thickness of the nose decreases. Interestingly, this result does not depend on H^*, a consequence of the fact that the nose of the very heavy current is thin, and hence the encountered ambient is, relatively, very deep. The leading coefficient of the effective Froude number χ is 2 which indicates that the heavy current tends to propagate much faster than could be anticipated from the Boussinesq counterpart value which is typically below 1. For $\rho_a/\rho_c \to 0$ the result (3.4) recovers the behaviour of the classical dam-break problem of a liquid (water) in a passive gas (air) (see Stansby *et al.* 1998 and Hogg & Pritchard 2004 where other references are also given).

Our results must be treated with care in the shallow ambient configuration $H^* < 2$. In this case there is a significant return flow in the ambient, which seems to be inconsistent with the one-layer dominance. However, we can argue that what is important is momentum (not volume) flux, and when ρ_c/ρ_a is large the momentum flux of the return flow is relatively small. In other words, we expect that the validity of the one-layer model improves as the heavy current departs from the Boussinesq case. Consider the worst case $H^* = 1$. Equation (3.3) yields the valid $h_N/h_0 < 1/2$ for $\rho_c/\rho_a > 1.373$, and the unacceptable $h_N/h_0 > 1/2$ for a smaller ρ_c/ρ_a. In the latter case it is necessary to impose the constraint $h_N/h_0 = 1/2$, which means that the flow is controlled (blocked or choked) by the front condition, i.e. by the right-hand side of (3.1). We thus obtain $\chi = 0.5(\rho_c/\rho_a)^{1/2}$ for $H^* = 1$ and $\rho_c/\rho_a < 1.373$. As H^* increases the $a = 1/2$ constraint must be applied to an even smaller range of ρ_c/ρ_a, and for

$H^* > 1.1$ (approximately) the solutions of (3.3) satisfy $a < 1/2$ straightforwardly. The major point is that the choking effect is a very restricted occurrence for the heavy current, in contrast with the light current discussed below. The present model is able to predict (approximately) the speed u_N and height h_N/h_0 in chocked circumstances (also for the light current), but does not resolve the mismatch between the sides of (3.1). This indicates that the interface of the chocked slumping current will readjust, most likely in accord with with the expansion-wave solution discussed by Lowe *et al.* (2005).

Light current. We rewrite (3.1) as

$$\left[1-\sqrt{\frac{h_N}{h_0}}\right]=\frac{1}{2}\left(\frac{\rho_c}{\rho_a}\right)^{1/2}\sqrt{\frac{h_N}{h_0}}Fr(a). \tag{3.5}$$

For a very light current $\rho_c/\rho_a \to 0$, the right-hand side becomes small, and in order to balance it h_N/h_0 on the left-hand side must approach 1. A formal expansion of h_N/h_0 in terms of the small parameter $(\rho_c/\rho_a)^{1/2}$ yields the leading terms approximation

$$\chi = Fr\left(\frac{1}{H^*}\right)\left[1-\sqrt{\frac{\rho_c}{\rho_a}}\left(\frac{1}{2}Fr\left(\frac{1}{H^*}\right)-\frac{|Fr'|}{H^*}\right)\right],\quad \frac{h_N}{h_0}=1-\sqrt{\frac{\rho_c}{\rho_a}}Fr\left(\frac{1}{H^*}\right),\quad \left(\frac{\rho_c}{\rho_a}\ll 1\right), \tag{3.6}$$

where $Fr' = \mathrm{d}Fr/\mathrm{d}a$ calculated at $a = 1/H^*$. The difference with the heavy current is evident. Here the results depend on the initial depth ratio H^*. For small ρ_c/ρ_a we obtain the interesting collapse of χ to Fr corresponding to the initial $h_0/H = 1/H^*$. The effective Froude number χ of the light current increases with the depth of the ambient H^* and its maximum is $\sqrt{2}$. The height of the front of the current tends to remain close to that of the lock, $h_N/h_0 \approx 1$.

The results (3.6) are clearly non-applicable to shallow ambients $H^* < 2$ (approximately) because the $h_N/h_0 \approx 1$ outcome violates the energy constraint $h_N/h_0 \leqslant (1/2)H^*$. Equation (3.5) shows that for $H^* < 2$ the flow becomes dominated by this constraint. This is in full agreement with the results of Lowe *et al.* (2005) and Birman *et al.* (2005) for the full-depth lock. Let us illustrate the pertinent result for the particular case $H^* = 1$. The thickness of the light current leaving the lock decreases, but must decrease more than predicted by (3.5), until the energy constraint is first fulfilled. This happens at $h_N/h_0 = H^*/2 = 1/2$. At this value the right-hand side of (3.1) (the nose condition) is smaller than the left-hand side (the intrinsic speed), and a further decrease of h_N will enhance the imbalance. The conclusion is that for $H^* < 2$ and a sufficiently small ρ_c/ρ_a the front discontinuity blocks the internal velocity of the current, i.e. the flow is choked at this half-channel thickness by the attainable speed of the nose. This can be generalized by the compact result (for the light current)

$$\chi = \frac{1}{2}\sqrt{H^*},\quad \frac{h_N}{h_0}=\frac{1}{2}H^*,\quad \left(H^* < 2, \frac{\rho_c}{\rho_a} < [4(1-\sqrt{H^*/2})]^2/H^*\right). \tag{3.7}$$

$H^* \to \infty$, *any* ρ_c/ρ_a. Here $a \to 0$ and hence $Fr(a) = \sqrt{2}$. Using this value in (3.1), and denoting $\sigma = [\rho_c/(2\rho_a)]^{1/2}$ we obtain after some algebra

$$\frac{h_N}{h_0} = (1+\sigma)^{-2},\quad \chi = \begin{cases} 2\sigma(1+\sigma)^{-1} & (\rho_c/\rho_a \geqslant 1) \\ \sqrt{2}(1+\sigma)^{-1} & (\rho_c/\rho_a \leqslant 1). \end{cases} \tag{3.8}$$

This remarkably simple exact solution of (3.1) predicts that in a deep ambient h_N/h_0 decreases from 1 to 0 as ρ_c/ρ_a increases from 0 to ∞, while χ first decreases from $\sqrt{2}$ to the minimum 0.83 at the Boussinesq limit $\rho_c/\rho_a = 1$, then increases to 2. We

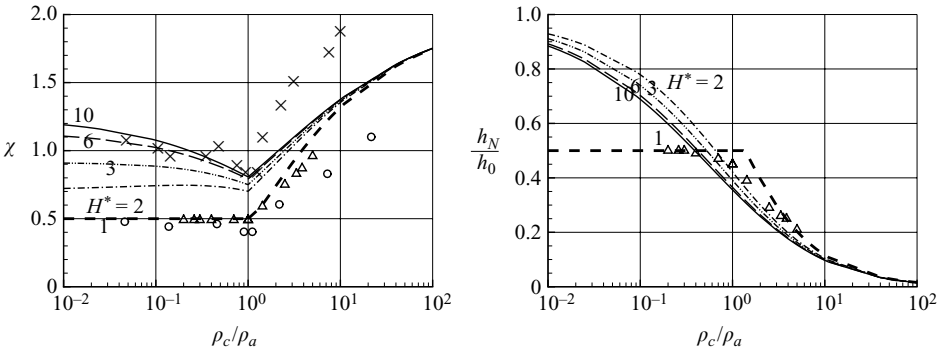

FIGURE 2. χ and h_N/h_0 as functions of ρ_c/ρ_a for various depth ratio $H^* = H/h_0$ (1, 2, 3, 6, 10). Symbols show experiments of Gröbelbauer *et al.* ($H^* = 1$ circles, $H^* = 6$ $\times$) and numerical simulations of Birman *et al.* ($H^* = 1$ triangles).

note that equations (20), (21) of Fanneløp & Jacobsen (1984) provide a similar result, except for the unspecified $Fr(0)$ (denoted $k^{1/2}$ in that paper).

3.2. *General results*

In general, (3.1) must be solved numerically for the unknown h_N/h_0, subject to $h_N/h_0 \leqslant (1/2)H^*$ as discussed above. The results for ρ_c/ρ_a in the range $[10^{-2}, 10^2]$ and for various H^* are displayed in figure 2. The symbols are data from Navier–Stokes simulations and experiments reported in previous studies, as specified in the caption.

This figure confirms and further elaborates the asymptotic trends discussed above. Indeed, except for a narrow range of density ratio about 1, there is a significant difference between the heavy and the light current. The heavy current displays a larger speed and a thinner front domain, and its features are less influenced by the depth ratio. The speed of the light current increases quite significantly with the thickness of the ambient. For $H^* = 1$ (relevant to <2) the light current is choked to occupy only half the thickness of the channel and moves with restricted speed, while the heavy current propagates mainly with unrestricted height and speed. For a given H^*, χ attains the minimum: (*a*) at the Boussinesq $\rho_c/\rho_a \approx 1$ for $H^* \geqslant 2$ and (*b*) on the light-current choked branch for $H^* < 2$.

The agreement with the numerical and experimental points is in general good. Unfortunately, only a very restricted comparison can be made. The present one-layer model is expected to be mainly relevant to values of H^* larger than 1, for which practically no data are available. As mentioned before, the most recent and accurate data are for the full-depth case $H^* = 1$. Gröbelbauer *et al.* (1993) presented some experimental data for $H^* = 6$ depth ratio release geometry. However, the currents were released by a partly lifted gate from a deep reservoir, not from a lock of part depth. Considering the motion of the backward-moving characteristics and rarefaction wave, we expect a significant difference between our theory and this type of experiment concerning the heavy current. Moreover, these experiments were performed with gases and may be affected by diffusion. Therefore these data (the $\times$ symbols in figure 2) may not be sufficiently relevant for a clear-cut quantitative comparison. But we find quite good quantitative agreement for $0.046 \leqslant \rho_c/\rho_a < 1.1$, and qualitative consistency for the other points.

It is interesting to note that, according to figure 2, the best support for the predictions of the model comes from parameter regimes where the momentum equation

of the model is expected to be least valid: (*a*) the full-depth $H^* = 1$ high-resolution numerical data (the triangles in figure 2); and (*b*) some of the deep light-current experimental results (the $\times$ symbols in figure 2 for $0.0463 \leqslant \rho_c/\rho_a \leqslant 0.334$, where $0.28 \leqslant H^* \rho_c/\rho_a \leqslant 2.0$). The agreement is remarkable. A plausible explanation is as follows. First, the discrepancy between the data and the model can be attributed to errors in the data. The data for $H^* = 1$ are the most accurate. We expect that comparisons with more accurate data for larger H^* will show better agreement. Second, figure 2 is concerned only with speed and height of the nose. A comparison of additional features of the current is expected to reveal, in general, better agreement at larger values of H^* (in particular for light currents which are prone to choking). Third, it is possible that the simple balances used in our model capture the governing physical mechanism better than suggested by the magnitude of the neglected terms (e.g. owing to internal cancellation of effects the global deviation is smaller than the local error). This conjecture requires further verification.

Overall, we think that a useful extension of the SW model has been achieved. The classical Boussinesq domain is just a very narrow strip about the line $\rho_c/\rho_a = 1$ in the parameter plane of figure 2.

4. Self-similar stage

After a significant propagation, the current 'forgets' the initial conditions, and a self-similar behaviour is expected. Now the current is sufficiently thin (or deep) so that $a \to 0$ and Fr at the front becomes constant. We define

$$\mathscr{F}^2 = \frac{\rho_c}{\rho_a} Fr^2(0) = 2\frac{\rho_c}{\rho_a}. \tag{4.1}$$

In this section we use dimensionless variables. For a rectangular lock we scale x, h, u, t by $x_0, h_0, (|\Delta\rho| g h_0/\rho_c)^{1/2}, x_0[\rho_c/(|\Delta\rho| g h_0)]^{1/2}$, respectively. In general in this scaling we can replace both x_0 and h_0 by $L = \mathscr{V}^{1/2}$ where $\mathscr{V}$ is the volume (per unit width). The solution of (2.1), (2.4) and nose boundary conditions is now

$$x_N(t) = At^{2/3}, \quad u = \dot{x}_N y, \quad h = \dot{x}_N^2 \left(c + \frac{1}{4} y^2\right), \quad c = \frac{1}{\mathscr{F}^2} - \frac{1}{4}, \quad (0 \leqslant y \leqslant 1), \tag{4.2}$$

where $y = x/x_N$, the overdot denotes the time derivative, and A is a constant. These results were also derived by Fanneløp & Jacobsen (1984) and Gratton & Vigo (1994) but with an unspecified value of $Fr(0)$. The similarity results are not sharp because initial conditions are not satisfied, and t can be replaced by $t + \text{Const}$ without invalidating them.

Both light and heavy currents propagate with $t^{2/3}$. There is, however, a difference in the expected shape. For very light currents the small $\mathscr{F}$ produces $c \gg 1$, and hence the profile is a spreading rectangle, $h \approx (2A/3)^2 c t^{-2/3}$, with a relatively small contribution from the y^2 term. The opposite structure, of a sharp tail-to-head difference, is expected for the very heavy current, as follows.

First, we note that c decreases when $\mathscr{F}$ increases. For $\rho_c/\rho_a > 2$ we obtain $\mathscr{F}^2 > 4$, and hence in this case h predicted by (4.2) is negative for $y < y_1$ where

$$y_1 = \left(1 - \frac{4}{\mathscr{F}^2}\right)^{1/2} = \left(1 - 2\frac{\rho_a}{\rho_c}\right)^{1/2}. \tag{4.3}$$

This result has been reported by Fanneløp & Jacobsen (1984) and Gratton & Vigo (1994) for a self-similar current with an unspecified $Fr(0)$ (here we use the specific (4.1)). These previous studies suggested that the negative h of the similarity result

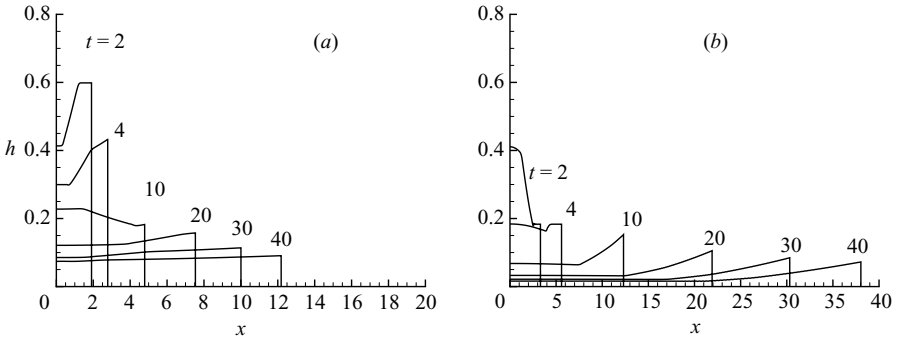

FIGURE 3. Propagation of (*a*) light $\rho_c/\rho_a = 0.25$ and (*b*) heavy $\rho_c/\rho_a = 4$ currents released from a rectangular lock with $H^* = 4$. Finite-difference solution of the SW equations.

means that the heavy current leaves behind a bare patch on the bottom, or an empty spot, in the region $x < y_1 A t^{2/3}$, approximately. However, the evolution of this peculiar shape for a realistic current released from behind a lock needs clarification. We observe that the region where the classic similarity result (4.2) yields a negative h is covered by a thin horizontal tail of the current. This corresponds to another branch of the long-time exact solutions of the SW equations (2.1) and (2.4), namely

$$h(x,t) = \frac{C}{t}, \quad u(x,t) = \frac{1}{t}x, \tag{4.4}$$

where C is a constant of order unity. The dam-break results indicate that this solution develops for small x during the transition from slumping to similarity phases. For a heavy current this inner solution spreads out and prevails for large times because it is able to coexist with the fast-moving nose. The self-similar profile for $\rho_c/\rho_a > 2$ combines the horizontal tail (4.4) for $0 \leqslant y < y_m$, and the prominent head (4.2) for $y_m \leqslant y < 1$, where $y_m \approx y_1$. This structure, and the evolution of different shapes for the heavy and light currents, is confirmed by the numerical solutions of the SW equations (using 200 grid points for $0 \leqslant y \leqslant 1$) displayed in figure 3. The volume of the fluid in the tail decays like $t^{-1/3}$, which justifies the simplification of a bare bottom left behind a very heavy current. We think that the appearance of such a structure may be verifiable in experiments (but viscous effects may eventually slow down the decay of the tail).

Finally, the constant A follows from the volume conservation in the y domain $[y_j, 1]$ where $y_j = 0$ for $\rho_c/\rho_a \leqslant 2$, or y_1 for a heavier current. This yields

$$A = \left[\tfrac{4}{9}\left(c(1-y_j) + \tfrac{1}{12}\left(1-y_j^3\right)\right)\right]^{-1/3}. \tag{4.5}$$

5. Concluding remarks

We have presented a compact shallow-water model for the high-Reynolds-number gravity current which covers a quite wide range of density ratio of current to ambient fluids, ρ_c/ρ_a, and of the depth ratio H^*, and contains no adjustable constants. We derived simple expressions for the asymptotic trends of the current concerning the initial propagation of very heavy and very light currents, and in shallow and very deep ambients. Self-similar solutions for large times are also presented and confirmed. The main advantage of the model is the mathematical simplicity.

The main deficiency is that the validity is largely untested. The theoretical predictions are in good agreement with available experimental and numerical simulations

data. The comparisons cover, unfortunately, a very restricted parameter range owing to lack of data. The plausible limitation of the model is $H^*(\rho_c/\rho_a) > 2$, but this has not been confirmed by the comparisons, and some valuable results were obtained for smaller values of this parameter. We noted that the best agreements were obtained for parameter regimes outside that limit, in which the model is expected to be least valid. Extended comparisons and clarifications, in particular by high-resolution numerical studies such as performed by Etienne *et al.* (2005) and Birman *et al.* (2005) for the $H^* = 1$ case, would be useful. The present model is able to predict (approximately) the speed and height of the nose in chocked circumstances, but does not provide the full details of the interface in these cases. The remedy could be the two-layer matching presented by Lowe *et al.* (2005).

The behaviour of the non-Boussinesq current in the transition from the slumping to the self-similar situation requires the numerical solution of the hyperbolic system of equations for h and u. The methodology used for the Boussinesq cases (see for example Bonnecaze, Huppert & Lister 1993; Ungarish & Zemach 2005) can be extended to the present problem. Real gravity currents are influenced by numerous effects which were neglected in the present theory, such as viscosity, diffusion, entrainment, instabilities and surface tension, which future investigations could address.

In spite of these limitations and uncertainties, the suggested theory is a useful tool for understanding and modelling the gravity current. As Boussinesq and non-Boussinesq light and heavy currents can be now treated in a unified form by a single simple formulation, the investigation of non-Boussinesq cases is expected to be promoted. The present model could be extended to more complex circumstances, in particular to axisymmetric and rotating configurations.

REFERENCES

Benjamin, T. B. 1968 Gravity currents and related phenomena. *J. Fluid Mech.* **31**, 209–248.

Birman, V. K., Martin, J. E. & Meiburg, E. 2005 The non-Boussinesq lock exchange problem. Part 2. High-resolution simulations. *J. Fluid Mech.* **537**, 125–144.

Bonnecaze, R. T., Huppert, H. E. & Lister, J. R. 1993 Particle-driven gravity currents. *J. Fluid Mech.* **250**, 339–369.

Etienne, J., Hopfinger, E. J. & Saramito, P. 2005 Numerical simulations of high density ratio lock-exchange flows. *Phys. Fluids* **17**, 036601-12.

Fanneløp, T. K. & Jacobsen, Ø. 1984 Gravity spreading of heavy clouds instantaneously released. *Z. Angew. Math. Phys.* **35**, 559–584.

Gratton, J. & Vigo, C. 1994 Self-similar gravity currents with variable inflow revisited: plane currents. *J. Fluid Mech.* **258**, 77–104.

Gröbelbauer, H. P., Fanneløp, T. K. & Britter, R. E. 1993 The propagation of intrusion fronts of high density ratios. *J. Fluid Mech.* **250**, 669–687.

Hogg, A. J. & Pritchard, D. 2004 The effects of hydraulic resistance on dam-break and other shallow inertial flows. *J. Fluid Mech.* **501**, 179–212.

Keller, J. J. & Chyou, Y.-P. 1991 On the hydraulic lock-exchange problem. *Z. Angew. Math. Phys.* **42**, 874–910.

Klemp, J. B., Rotunno, R. & Skamarock, W. C. 1994 On the dynamics of gravity currents in a channel. *J. Fluid Mech.* **269**, 169–198.

Lowe, R. J., Rottman, J. W. & Linden, P. F. 2005 The non-Boussinesq lock exchange problem. Part 1. Theory and experiments. *J. Fluid Mech.* **537**, 101–124.

Stansby, P. K., Chegini, A. & Barnes, T. C. D. 1998 The initial stages of dam-break flow. *J. Fluid Mech.* **374**, 407–424.

Ungarish, M. & Zemach, T. 2005 On the slumping of high Reynolds number gravity currents in two-dimensional and axisymmetric configurations. *Euro. J. Mech.* B/*Fluids* **24**, 71–90.